Int. J. Sci. R. Tech., 2026 3(9)
A Multidisciplinary peer-reviewed Journal
www.ijsrtjournal.com [ISSN: 2394-7063]

Original Article

A Research On Design And Synthesis Of Fused Heterocyclic Imidazothiazole And Benzothiazole Analogous As Potential Anti-Cancer Agents

Sakshi*, N. S. Gill, Surinderjeet Kaur

Department of Pharmaceutical Chemistry, Rayat Institute of Pharmacy, LSU.

ABSTRACT

Cancer remains a major global health challenge, creating a continued need for safer and more effective therapeutic agents. Since chronic inflammation is closely associated with cancer development and progression, compounds with both anticancer and anti-inflammatory properties are of particular interest. Chemical analogues are structurally modified compounds designed to improve properties such as biological activity, solubility, selectivity, and safety. Among various heterocyclic scaffolds, benzothiazole and imidazothiazole derivatives have attracted considerable attention because of their diverse biological activities and favorable interactions with biological targets. The presence of heteroatoms within these fused-ring systems can contribute to their pharmacological properties and target-binding ability. Accordingly, the development of new benzothiazole- and imidazothiazole-based compounds may provide useful candidates with dual anticancer and anti-inflammatory activity. Several approaches, including one-pot reactions, microwave-assisted synthesis, and environmentally friendly/green chemistry methods, have been explored for the preparation of such heterocyclic compounds. The present study therefore focuses on the design and synthesis of novel heterocyclic derivatives with the aim of investigating their potential as anticancer and anti-inflammatory agents.

Keywords: Benzothiazole, Imidazothiazole, Fused heterocycles, Anticancer activity, heteroatoms.

INTRODUCTION

Cancer is a major global health concern and remains one of the leading causes of death worldwide. Its increasing incidence is placing a growing burden on healthcare systems. Several lifestyle and environmental factors, including unhealthy dietary habits, physical inactivity, tobacco use, alcohol consumption, and exposure to harmful agents, can contribute to cancer risk. Among the molecular factors involved in cancer development, epidermal growth factor receptor (EGFR) is particularly important. Abnormal EGFR activation, overexpression, or mutation can promote cell proliferation, survival, and tumor progression. Dysregulated EGFR signaling has been associated with several common cancers, including lung, breast, colorectal, and head and neck cancers. Therefore, EGFR represents an important molecular target for the development of new anticancer agents.

Epidermal growth factor receptor (EGFR) belongs to the ErbB family of receptor tyrosine kinases, which includes ErbB1 (EGFR), ErbB2, ErbB3, and ErbB4. These receptors regulate important cellular processes such as growth, proliferation, survival, and differentiation. Abnormal EGFR signaling has been linked to several diseases, including inflammation and cancer. EGFR is frequently overexpressed or dysregulated in cancers such as breast, lung, non-small-cell lung, bladder, and head and neck cancers. Consequently, EGFR has become an important target in anticancer drug research. EGFR inhibitors act by reducing receptor tyrosine kinase activity and thereby interfering with downstream signaling pathways involved in cancer-cell growth and survival. Heterocyclic compounds are organic molecules with at least one carbon atom and at least one additional heteroatom, such as N, O, or S, that play an important part in the metabolism of living cells. It may be either nonaromatic or aromatic. Most of them are five or six membered and some of the rings contain higher than that of three, four, seven or larger rings. Fused

Relevant conflicts of interest/financial disclosures: The authors declare that the research was conducted in the absence of any commercial or financial relationships that could be construed as a potential conflict of interest.

heterocyclic compounds, which generally have five or six members, have sparked a lot of interest in medicinal chemistry because of their wide range of pharmacological and therapeutic implications.

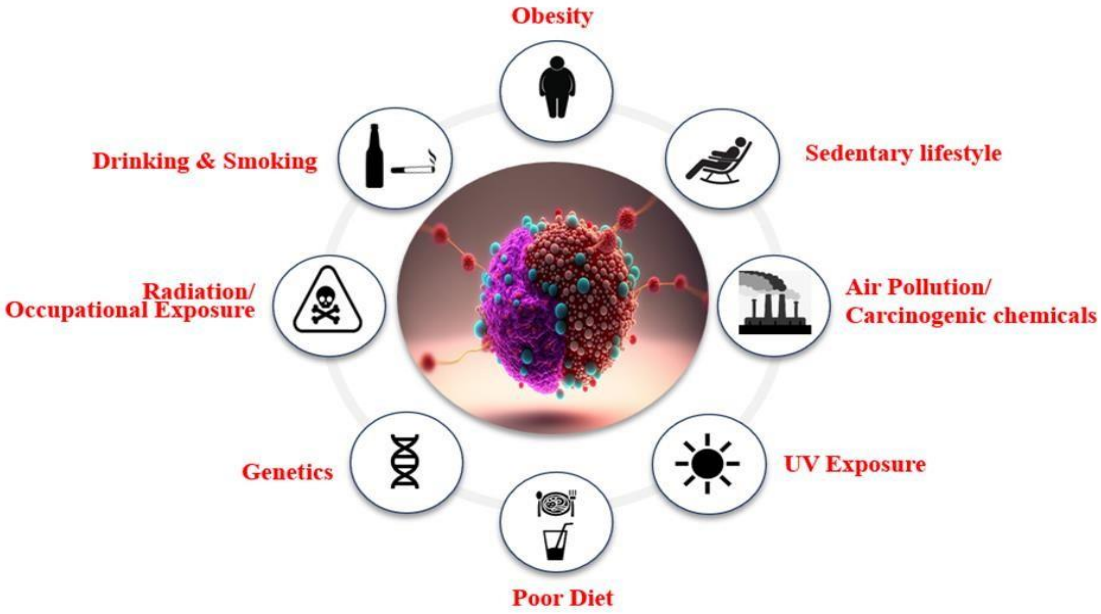

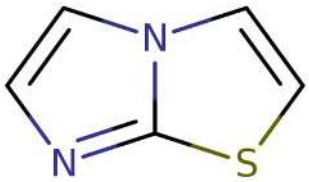

Imidazothiazole

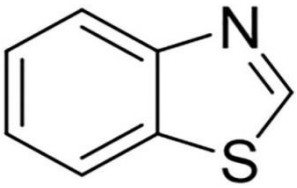

Benzothiazole

MATERIALS AND METHODS

All reagents and solvents used in the study were of laboratory grade and obtained from Merck (Darmstadt, Germany) and S.D. Fine Chemicals (Delhi, India). Reaction progress and compound purity were monitored by TLC using silica gel 60 F254 plates and suitable solvent systems. The spots were visualized under UV light and in an iodine chamber.

Melting points were determined using a Labtronics Digital Auto Melting Point Apparatus and were uncorrected. IR spectra were recorded using a Perkin-Elmer 1720 FTIR spectrometer. **^{1}H and ^{13}C NMR spectra** were recorded on Bruker Avance instruments using $CDCl_3$ or DMSO-d_6, with TMS as the internal standard. Chemical shifts were reported in ppm and coupling constants (*J*) in Hz. ESI-MS data were obtained using a Synapt G2 HDMS (Waters) instrument. Elemental analysis for C, H, and N was performed using a CHNS Vario EL III analyzer, with values within ±0.4% of the calculated results.

General procedure for the synthesis of compounds

An equimolar amount of Schiff base (3a–l, 10 mmol) and thioglycolic acid (20 mmol) was dissolved in 1,4-dioxane (25 mL), followed by the addition of a catalytic amount of anhydrous zinc chloride. The reaction mixture was stirred at room temperature for 16–20 h, and its progress was monitored by TLC. After completion, the mixture was poured onto crushed ice. The resulting solid was filtered, washed with water, dried, and finally recrystallized from ethanol to obtain the desired product.

SYNTHETIC SCHEME

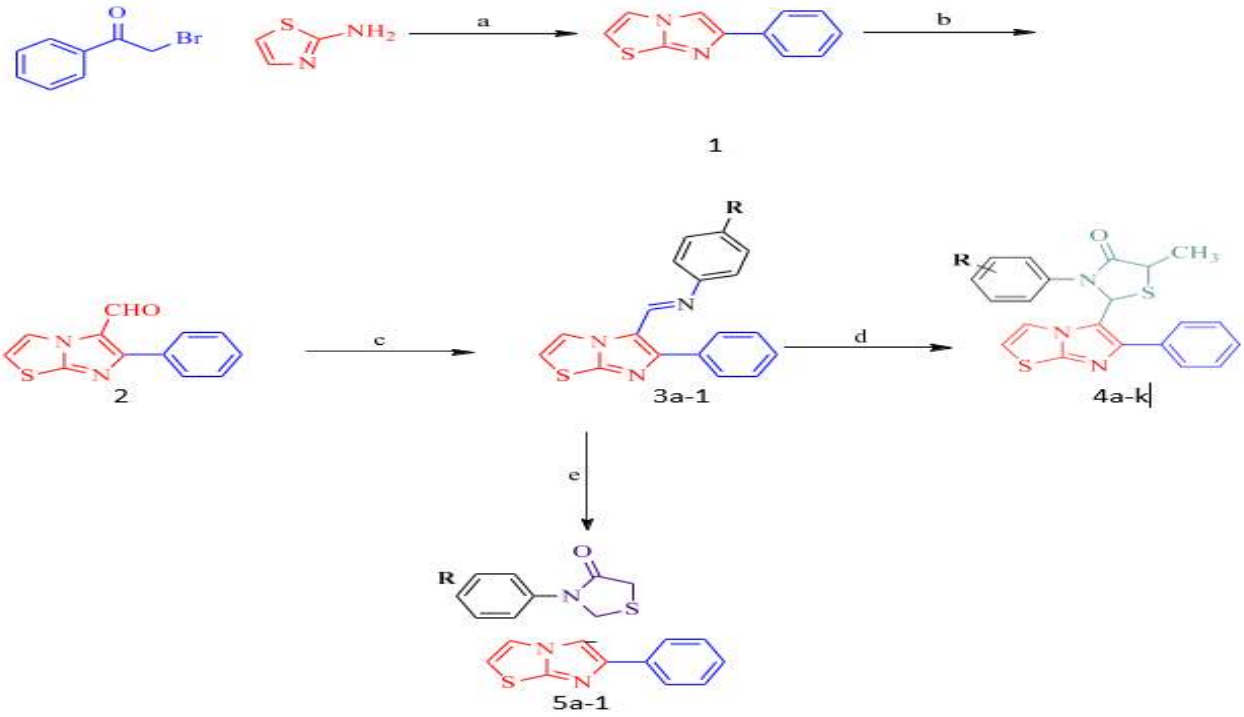

Scheme 1. Reagent and Conditions. (a) Methanol, 70 °C, Reflux, (b) $CHCl_3$, DMF, $POCl_3$, 120 °C, Reflux, (c) Substituted aniline, Toluene, PTSA, 120°C, (d) Thiolactic acid, 1-4 dioxane (e) Thioglycolic acid, 1-4 dioxane

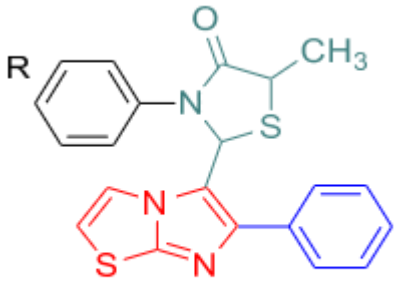

4a-k

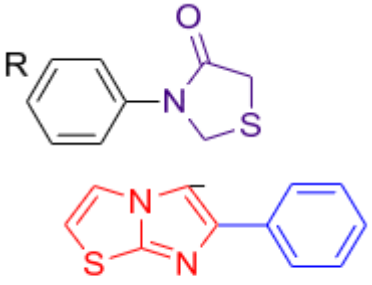

5a-1

Compounds	R
4a	2-Fluoro
4b	4-Fluoro
4c	2-Chloro
4d	4-Chloro
4e	2-Bromo
4f	4-Bromo
4g	2,4-Dichloro
4h	4-Nitro
4i	4-tolyl
4j	2-Methoxy
4k	4-Methoxy
5a	2-Fluoro
5b	4-Fluoro

Table. List of derivatives synthesised

3-(2-Fluorophenyl)-5-methyl-2-(6-phenylimidazo[2,1-b]thiazol-5-yl)thiazolidin-4-one(4a)

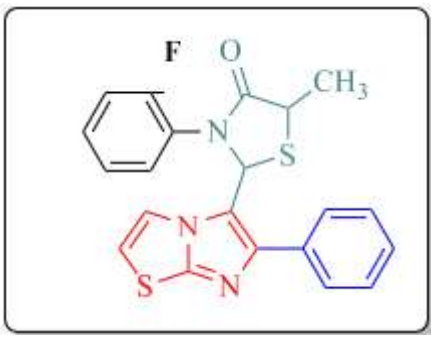

White powder, yield:69%, m.p. 170-172°C; IR(KBr, υ max cm^{-1}): 1689(C=O),1575(C=N), ^{1}HNMR (500MHz,DMSO-*d6*) δ1.52 (3H,d,*J*=7Hz,CH_3), 3.81 (1H,q,*J*=7Hz,CH), 5.88(1H,s,CH),6.79-7.90 (11H,complexm,9Ar-H&2CH=CH) ^{13}CNMR (125MHz, DMSO-*d6*) :21.51(CH_3), 43.08(CH), 63.71 (CH of thiazolidinones), 115.69, 116.11, 119.68, 120.93, 124.12, 124.16, 125.31, 126.61, 126.86, 128.19, 128.35, 129.23, 133.07, 140.51, 148.90, 155.78, 157.74, 172.96. HRMS-ESIm/z:calcd for $C_{21}H_{16}FN_3OS_2[M+H]^+$ 410.0719, found 410.0732; anal.calcd for C, 61.60; H, 3.94; N, 10.26; found: C, 61.77; H, 3.68; N, 10.03.

***4-Fluorophenyl)-5-methyl-2-(6-phenylimidazo[2,1-b]thiazol-5-yl)thiazolidin-4-one*(4b)**

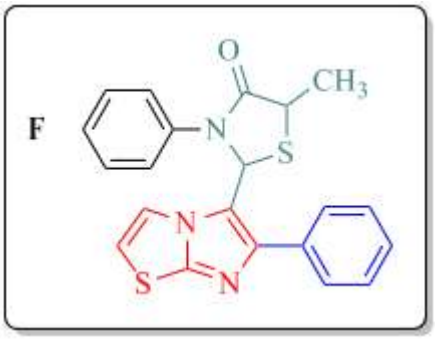

White solid, yield:72%, m.p.165-167°C; IR (KBr,υ maxcm^{-1}): 1687(C=O), 1560(C=N), ^{1}HNMR (500MHz, DMSO-*d6*) δ1.19(3H, d,*J*=7Hz, CH_3),3.45(1H, q, *J*=7Hz, CH), 6.06 (1H, s, CH), 7.13-7.69 (11H, complex m, 9Ar-H & 2 CH=CH),^{13}C NMR (125 MHz, DMSO-*d6*): 21.26 (CH_3), 43.18(CH), 63.93(CH of thiazolidinones),112.17, 121.55, 122.72, 124.15, 125.96, 128.55, 128.77, 129.25, 130.25, 135.06, 138.14, 143.12, 145.41, 146.11, 156.72, 171. 33; HRMS-ESI m/z: calcd for $C_{21}H_{16}FN_3OS_2[M+H]^+$410.0719, found 410.0715;anal. Calcd for C,61.60; H, 3.94; N,10.26; found: C, 61.71;H, 4.12; N, 10.35.

***3-(2-Chlorophenyl)-5-methyl-2-(6-phenylimidazo[2,1-b]thiazol-5-yl)thiazolidin-4-one*(4c)**

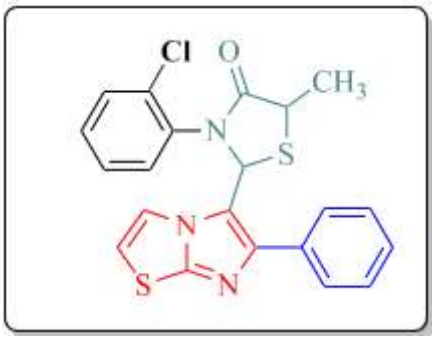

Grey powder, yield:67%, m.p.164-166°C; IR (KBr, υ maxcm^{-1}): 1674(C=O), 1571(C=N), ^{1}HNMR (500MHz, DMSO-*d6*) δ1.29 (3H, d, *J*=7Hz, CH_3), 3.74(1H, q, *J*=7Hz, CH), 5.93(1H, s, CH), 7.28-7.84 (11H, complex, 9 Ar-H & 2CH=CH) ^{13}CNMR (125MHz, DMSO-*d6*): 19.09 (CH_3), 42.90 (CH), 64.30 (CH of thiazolidinones), 116.11, 119.85, 120.61, 120.93, 121.30, 122.30, 123.71, 126.61, 129.23, 129.70, 130.30, 133.07, 135.07, 138.60, 140.49, 148.90, 153.34, 173.58. HRMS-ESIm/z: calcd for $C_{21}H_{16}ClN_3OS_2[M+H]^+$ 426.0423, found 426.0427, 427.0541$[M+2]^+$; anal.calcd for C, 59.22; H, 3.79; N, 9.87; found:C, 59.41; H, 3.66; N, 9.63.

***3-(4-Chlorophenyl)-5-methyl-2-(6-phenylimidazo[2,1-b]thiazol-5-yl)thiazolidin-4-one*(4d)**

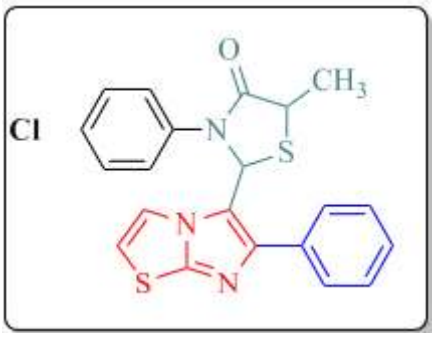

White powder, yield:78%, m.p.177-179°C; IR (KBr,υmax cm^{-1}): 1682(C=O), 1575(C=N), ^{1}HNMR (500 MHz, DMSO-d_6) δ1.11(3H, d, *J*=7Hz, CH_3), 3.51(1H, q, *J*=7Hz, CH), 6.06 (1H, s, CH), 7.17 – 7.69 (11H, complex m, 9Ar-H & 2 CH=CH),^{13}C NMR (125 MHz, DMSO-*d6*): δ21.25, (CH_3), 47.60 (CH),

60.63 (CH of thiazolidinones), 112.89, 120.95, 121.10, 121.42, 124.10, 125.44, 125.95, 128.61, 129.39, 129.84, 131.14, 138.34, 145.82, 152.56, 154.34, 173.47. HRMS-ESIm/z: calcd for $C_{21}H_{16}ClN_3OS_2[M+H]^+$426.0423, found 426.0427, 427.0392 $[M+2]^+$; anal.calcd for C, 59.18; H, 3.79; N, 9.87; found: C, 59.21; H, 3.81; N, 9.75.

***3-(2-Bromophenyl)-5-methyl-2-(6-phenylimidazo[2,1-b]thiazol-5-yl)thiazolidin-4-one*(4e)**

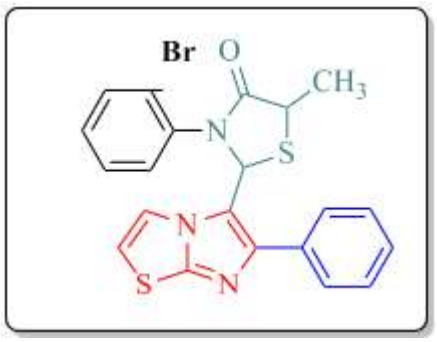

Light brown powder, yield: 71%, m.p. 169-171°C; IR (KBr, υmax cm^{-1}): 1684 (C=O), 1571 (C=N), ^{1}H NMR (500 MHz, DMSO-*d6*) δ 1.21 (3H, d, *J* = 6 Hz, CH_3), 3.72 (1H, q, *J* = 7.5 Hz,CH), 5.79 (1H, s, CH), 6.85-7.71 (11H, complexm, 9Ar-H & 2CH=CH), ^{13}CNMR (125MHz, DMSO-*d6*): 19.09(CH_3), 42.15(CH), 63.82(CH of thiazolidinones), 116.11, 119.73, 120.21, 120.93, 126.61, 126.95, 129.23, 129.70, 129.73, 130.84, 131.67, 133.07, 133.84, 135.23, 136.50 , 140.49, 148.90, 172.87; HRMS-ESIm/z:calcd for $C_{21}H_{16}BrN_3OS_2$ $[M+H]^+$469.9918, found 469.9930, 470.9941$[M+2]^+$; anal.calcd for C, 53.62; H, 3.43; N, 8.93; found: C, 53.81; H, 3.17; N, 8.64.

***3-(4-Bromophenyl)-5-methyl-2-(6-phenylimidazo[2,1-b]thiazol-5-yl)thiazolidin-4-one*(4f)**

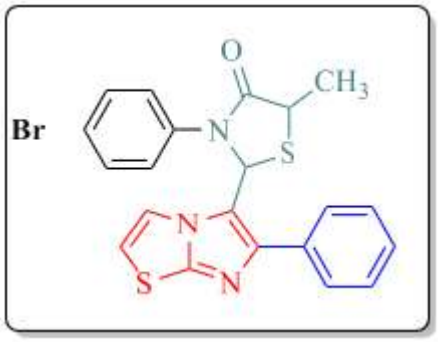

Yellow solid, yield: 78%, m.p. 172-174°C; IR spectra (KBr, υmax cm^{-1}): 1672 (C=O), 1568 (C=N), ^{1}H NMR (500 MHz, DMSO-*d6*): δ1.12 (3H, d, *J* = 7 Hz,CH_3), 3.22 (1H, q, *J* = 7Hz, CH), 6.05 (1H, s, CH), 7.10-7.98 (11H, complexm, 9Ar-H & 2CH=CH), ^{13}CNMR, 125MHzDMSO-d_6)20.02(CH_3), 42.92(CH), 66.82 (CH of thiazolidinones), 117.71, 119.72, 120.33, 121.60, 124.58, 124.96, 125.96, 128.17, 128.52, 129.04, 129.39, 130.29, 137.83, 144.41, 144.90, 178.58. HRMS(ESI)m/z:calcd for $C_{21}H_{16}BrN_3OS_2[M+H]^+$ 469.9918 found 469.9915, 470.9897$[M+2]^+$; anal. calcd for C, 53.62; H, 3.43; N, 8.93; found: C, 53.57; H, 3.51; N, 9.11.

***3-(2,4-Dichlorophenyl)-5-methyl-2-(6-phenylimidazo[2,1-b]thiazol-5-yl)thiazolidin-4-one* (4g)**

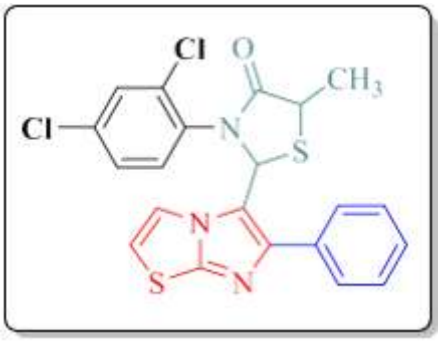

Yellow solid, yield:67 %,m.p. 151-153 °C; IR (KBr, υmax cm^{-1}): 1678 (C=O), 1563 (C=N), ^{1}H NMR (500 MHz, DMSO-*d6*): δ1.18 (3H, d, *J* = 5Hz, CH_3), 4.13 (1H, q, *J* =5Hz, CH), 5.02 (1H, s, CH), 7.03-8.27 (10 H, complex m, 8Ar-H & 2 CH=CH),^{13}C NMR (125MHz, DMSO-*d6*):δ21.24, (CH_3)42.88, (CH), 60.48 (CH of thiazolidinone), 119.87, 120.32, 121.59, 122.04, 123.98, 124.47, 125.96, 128.62, 129.40, 130.01, 138.38, 144.09, 144.41, 155.60, 156.86, 178.56, (C=O); HRMS(ESI)m/z:calcd for $C_{21}H_{15}Cl_2N_3OS_2[M+H]^+$ 460.0034 found 460.0031, 461.0001$[M+2]^+$; anal.calcd for C,54.79; H, 3.28; N, 9.13; found: C, 54.87; H, 3.37; N, 9.18.

***4-Methyl-3-(4-nitrophenyl)-2-(6-phenylimidazo[2,1-b]thiazol-5-yl)thiazolidin-4-one*(4h)**

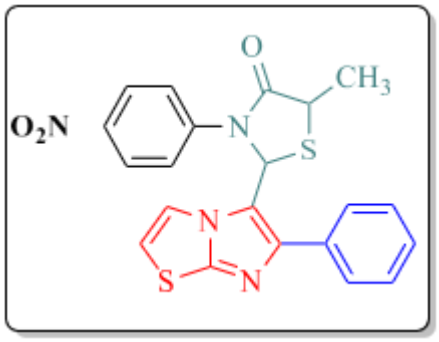

Off-white powder, yield: :72%; m.p.187-189°C; IR(KBr, cm-1):1684(C=O),1571(C=N), ^{1}HNMR(500MHz, DMSO-*d6*) δ1.49 (3H, d, *J*=5.2Hz, CH_3), 4.12(1H, q, *J*=5.1, Hz CH), 5.02 (1H, s, CH), 7.49- 8.27 (11H, complex m, 9Ar-H & 2 CH=CH), ^{13}C NMR (125 MHz, DMSO-*d6*):21.67(CH_3), 47.62(CH)63.25 (CH of thiazolidinones), 114.87, 116.81, 117.92, 119.25, 119.50, 120.49, 125.97, 128.11, 128.27, 128.34, 128.57, 129.13, 138.21, 144.24, 150.02, 175.14 (C=O) HRMS(ESI)m/z:Calcd. For $C_{21}H_{16}N_4O_3S_2$[M+H]$^+$437.0664 found 437.0667; anal.calcd for C, 57.78; H, 3.69; N, 12.84; found:C, 57.89; H, 3.76; N, 11.71.

***5-Methyl-2-(6-phenylimidazo[2,1-b]thiazol-5-yl)-3-p-tolyl)thiazolidin-4-one*(4i)**

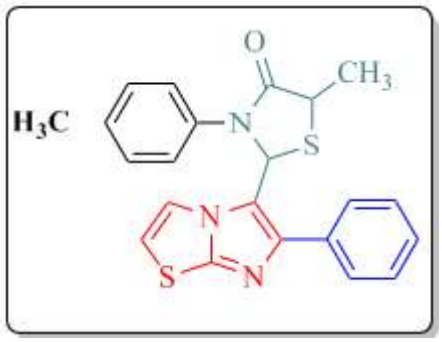

Yellow solid, yield:67%, m.p.155-157°C; IR (KBr, υmaxcm^{-1}): 1685(C=O), 1565 (C=N), ^{1}HNMR (500MHz, DMSO-*d*$_6$) δ1.47(3H, d, *J*=5.5Hz, CH_3), 2.61(3H, s, CH_3), 4.11(1H, q, *J*=5.5Hz, CH),5.02(1H, s, CH),7.42-8.23(11H, complexm, 9Ar-H&2 CH=CH), ^{13}CNMR (125MHz, DMSO-*d*$_6$) δ17.39, (CH_3)21.25(CH_3)47.29, (CH)66.81, (CH of thiazolidinone) 110.52, 112.89, 115.60120.95, 121.10, 121.42, 124.10, 125.44, 125.95, 128.61, 129.39, 129.84, 138.34, 145.82, 152.56, 173.47: HRMS(ESI)m/z:Calcd for $C_{20}H_{19}N_3OS_2$[M+H]$^+$406.0970 found 406.0987; anal.calcdforC, 65.16; H,4.72; N, 10.36; found: C, 65.29; H, 4.84; N, 10.43.

***3-(2-Methoxyphenyl)-5-methyl-2-(6-phenylimidazo[2,1-b]thiazol-5-yl)thiazolidin-4-one*(4j)**

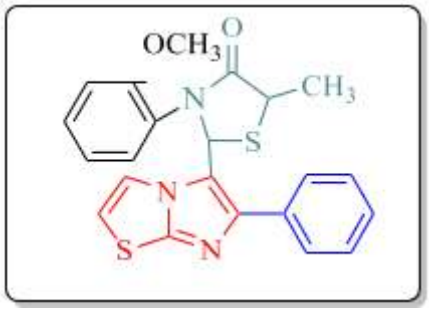

Yellow powder, yield: 73%, m.p. 171-173°C; IR (KBr, υmax cm^{-1}): 1673 (C=O), 1569 (C=N), ^{1}H NMR (500 MHz, DMSO-*d6*) δ 1.25 (3H, d, *J* = 7.5Hz, CH_3), 3.57 (1H, q, *J* = 7.5Hz, CH) 3.69 (3H, s, OCH_3), 5.84 (1H, s, CH), 6.55 -7.71 (11H, complex m, 9Ar-H & 2 CH=CH).^{13}CNMR(125MHz,DMSO-*d6*):19.10(CH_3),43.02(CH),55.08(CH of thiazolidinones), 63.71(CH_3), 113.62, 116.11, 119.56, 119.81, 120.93, 123.83, 124.38, 126.61, 129.12, 129.23, 129.70, 133.06, 135.61, 140.52, 148.90, 152.85, 173.07. HRMS-ESI m/z:calcd for $C_{22}H_{19}N_3O_2S_2$[M+H]$^+$422.0919, found 422.0935; anal.calcd for C, 62.69; H, 4.54; N, 9.97; found: C, 62.45; H, 4.80; N, 10.08.

***3-(4-Methoxyphenyl)-5-methyl-2-(6-phenylimidazo[2,1-b]thiazol-5-yl)thiazolidin-4-one* (4k)**

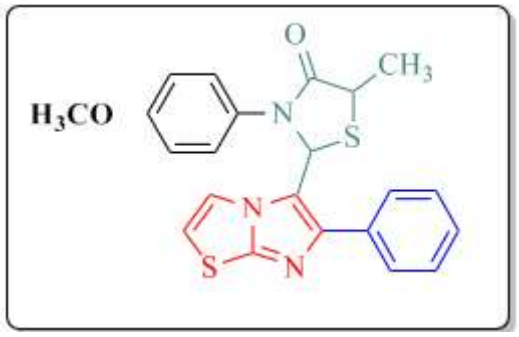

Yellow solid, yield:67%, m.p.162-164°C; IR (KBr, υmaxcm^{-1}):1690(C=O),1573(C=N), ^{1}HNMR (500 MHz, DMSO-*d*$_6$) δ1.12(3H,d, *J*=7.5Hz,CH_3), 3.45 (1H,q, *J*=7.5Hz, CH) 3.56(3H, s, OCH_3), 6.05(1H, s, CH), 6.92–7.97(11H, complexm, 9Ar-H & 2CH=CH), ^{13}CNMR(125MHz, DMSO-*d*$_6$)20.91,

(CH_3), 42.91(CH), 60.62(CH of thiazolidinone), 63.24(CH_3), 114.12, 118.81, 119.02, 120.06, 120.30, 122.88, 125.96, 128.59, 128.96, 130.25, 130.61, 133.90, 144.11, 145.61, 159.81, 173.31: HRMS(ESI)m/z:Calcd for: $C_{22}H_{19}N_3O_2S_2[M+H]^+$422.0919 found 422.0915; anal.calcd for C, 62.69; H, 4.54; N, 9.97; found: 62.51; H, 4.67; N, 10.08.

***3-(2-Fluorophenyl)-2-(6-phenylimidazo[2,1-b]thiazol-5-yl)thiazolidin-4-one*(5a)**

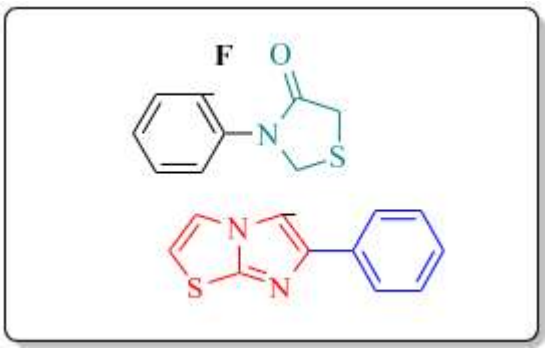

Yellow powder, yield: 75%, m.p.170-172°C; IR (KBr, υmaxcm^{-1}):1679(C=O),1583 (C=N), ^{1}HNMR (500MHz, DMSO-*d6*) δ3.73(1H, d, *J*=6Hz, CH_2 thiazolidinone), 3.85 (1H, d, *J* = 6 Hz, CH_2 thiazolidinone), 5.43 (1H, s, CH), 6.89 -7.97 (11H, complex m, 9Ar-H &2CH=CH). ^{13}CNMR (125MHz, DMSO-*d6*) : 33.58 (CH_2), 61.52(CH), 115.69, 116.11, 120.95, 123.94, 123.98, 125.32, 125.38, 126.83, 126.86, 128.70, 128.86, 129.23, 133.07, 141.04, 148.90, 155.65, 157.61, 170.71. HRMS-ESIm/z:calcd for $C_{20}H_{14}FN_3OS_2[M+H]^+$ 396.0562, found 396.0571; anal.calcd for C, 60.74; H, 3.57; N, 10.63; found: C, 61.28; H, 3.78; N, 10.44.

***3-(4-Fluorophenyl)-2-(6-phenylimidazo[2,1-b]thiazol-5-y)thiazolidin-4-one*(5b)**

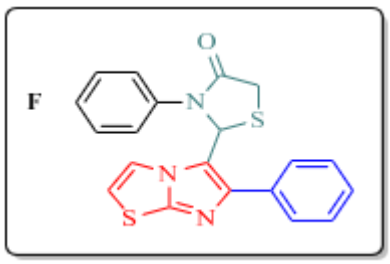

Yellow powder, yield:67%, m.p.152-154°C; IR (KBr, υmaxcm^{-1}):1685(C=O),1579(C=N), ^{1}HNMR (500MHz, DMSO-*d6*): δ3.51(1H, d, *J*=6Hz,CH_2 thiazolidinone), 3.65(1H, d, *J*= 6, CH_2 thiazolidinone), 5.39(1H, s, CH), 6.98-8.18 (11H, complexm, 9Ar-H & 2CH=CH). ^{13}CNMR (125MHz, DMSO-*d6*): δ33.73(CH_2), 63.56(CH), 109.41, 115.11, 116.48, 116.66, 123.30, 128.59, 128.69, 129.46, 129.53, 131.99, 134.90, 137.86, 143.90, 144.67, 155,41, 161.60, 163.57, 173.18 HRMS(ESI)m/z:calcd. for: $C_{20}H_{14}FN_3OS_2[M+H]^+$396.0562 found 396.0575; anal. calcd. for: $C_{20}H_{14}FN_3OS_2C$, 60.74; H,3.57; N, 10.63; found: C, 60.57;H, 3.31; N, 10.47.

***n-vitro* studies**

***In vitro* anti-cancer assay**

The cytotoxic activity of the synthesized derivatives was evaluated using the MTT colorimetric assay. The compounds were tested against A549 (lung), MCF-7 (breast), and HCT-116 (colon) cancer cell lines, along with HEK-293 cells as a normal cell line. Cells were seeded in 96-well plates at 3 × 10³ cells/well and incubated for 24 h. The test compounds were then added at concentrations of 10, 20, 40, and 80 µM and incubated for 72 h. MTT solution (100 µL) was subsequently added and the plates were incubated at 37 °C for 5 h. The resulting formazan crystals were dissolved in DMSO, and absorbance was measured at 570 nm using an ELISA reader. Each experiment was performed in triplicate, and IC_{50} values were calculated using GraphPad Prism and Microsoft Excel.

***In-vitro* EGFR kinase assay**

The synthesized compounds were evaluated for their ability to inhibit EGFR tyrosine kinase activity using A549 human lung cancer cells, which express high levels of EGFR. A549 cells were seeded in 24-well plates at 5 × 10³ cells/well and treated with different concentrations of the test compounds (0.2–500 µM) in triplicate. Following treatment, the cells were washed with cold PBS and lysed using HNTG buffer. The lysates were centrifuged at 15,000 × g for 12 min, and the collected supernatants were used for EGFR estimation by ELISA. The plate wells were coated with the lysates and kept overnight at 4 °C. After blocking with 1% BSA, the wells were washed and incubated with diluted mouse serum followed by phospho-EGFR antibody. After further washing, *o*-phenylenediamine dihydrochloride substrate was added and allowed to react for 30 min. Absorbance

was recorded at 490 nm using an ELISA plate reader. The percentage inhibition was calculated as:

% Inhibition = [(Mean OD untreated − Mean OD treated) / Mean OD untreated] × 100

Wound Healing assay

The wound-healing assay was conducted using A549 cells. Cells were seeded in six-well plates at 5×10^5 cells/well and allowed to form a confluent monolayer for 24 h. A sterile 200 µL pipette tip was then used to create a straight scratch across the cell layer. The wells were washed with PBS to remove detached cells and treated with the selected concentrations of compounds 4b and 4c. Images of the scratched areas were captured at 0 and 24 h using a Nikon phase-contrast microscope, with two to three randomly selected fields examined for each treatment.

Nuclear Staining

Cellular nuclear morphology was examined by DAPI staining and fluorescence microscopy**.** Approximately 3×10^4 cells were seeded on coverslips in 24-well plates containing DMEM supplemented with 10% FBS and incubated for 24 h. The cells were then treated with the test compounds at their respective IC_{50} concentrations and incubated for 48 h. After treatment, the cells were washed with PBS and fixed with 4% paraformaldehyde for 10 min**.** The fixed cells were stained with freshly prepared DAPI solution in the dark for 10 min, followed by gentle PBS washing. Coverslips were mounted on glass slides using DPX and examined under a Nikon fluorescence microscope at 40× magnification using an appropriate blue/cyan filter.

Acridine orange-ethidium bromide staining

A549 cells were seeded in six-well plates at 4×10^4 cells/well and exposed to GO-AuNPs at concentrations of 1.56 and 12.5 µg/mL for 48 h. Following treatment, the cells were collected and stained with an acridine orange/ethidium bromide (AO/EtBr) mixture (1:1, v/v; 100 µg/mL in PBS). The stained cells were then examined under a fluorescence microscope to assess cellular and nuclear morphological changes.

BSA denaturation inhibition assay

The anti-inflammatory activity of the synthesized compounds was assessed using the albumin denaturation method, with diclofenac sodium as the reference drug. The test compounds and standard were dissolved in DMF and diluted with phosphate buffer (pH 7.4). A 1 mL test solution (100 µg/mL) was mixed with 1 mL of 1% albumin solution and incubated at 27 ± 1 °C for 15 min. Protein denaturation was induced by heating the mixtures at 60 °C for 10 min in a water bath. After cooling, absorbance was measured at 660 nm using a UV–Visible spectrophotometer. The assay was performed in triplicate.

The percentage inhibition of albumin denaturation was calculated as:

% Inhibition = $[(A_t/Ac) - 1] \times 100$

where A_t represents the mean absorbance of the test sample and Ac represents the mean absorbance of the control.

DPPH antioxidant assay

The in-vitro antioxidant activity of the synthesized compounds was evaluated using the DPPH radical scavenging assay, with BHA as the reference standard. A DPPH methanolic solution (0.5 mL, 0.3 mM) was mixed with the test compound solutions (1 mM) to obtain a final reaction volume of 3 mL. The mixtures were kept at room temperature for 30 min, after which absorbance was measured at 520 nm using a UV–Visible spectrophotometer. The antioxidant activity was expressed as percentage inhibition.

% Activity = [1 − (Absorbance of test / Absorbance of control)] × 100

Biological Screening

***In vitro* cytotoxicity**

The synthesized imidazothiazole–thiazolidinone derivatives 4a–k and 5a–l were screened *in vitro* against A549, MCF-7, and HCT116 human cancer cell lines using the MTT assay. The compounds showed moderate to good cytotoxic activity, with IC_{50} values ranging from 10.74 to 89.92 µM, while erlotinib was used as the reference drug.

Among the tested derivatives, 4f showed the highest activity against A549 cells (IC_{50} = 10.74 ± 0.40 µM), followed by 4d (21.06 µM) and 4b (22.52 µM). Against MCF-7 cells, compounds 4f and 4b exhibited IC_{50} values of 18.73 ± 0.88 and 22.76 µM, respectively. For HCT116 cells, 4f and 4b were the most active derivatives, with IC_{50} values of 23.22 ± 1.89 and 23.69 µM, respectively. Compounds 4b, 4d, and 4f were further investigated for EGFR kinase inhibition and cytotoxicity toward normal HEK293 cells. Among these, 4f showed the most promising overall profile, with IC_{50} values of 10.74, 18.73, and 23.22 µM against A549, MCF-7, and HCT116 cells, respectively. It also showed comparatively lower toxicity toward HEK293 cells, with an IC_{50} of 96.38 ± 1.79 µM, suggesting better selectivity toward cancer cells.

Compounds	**R**	**IC_{50}(µM)(Mean± SD) ***		
		A549	**MCF7**	**HCT116**
4a	2-Fluoro	30.09 ± 3.85	41.03 ± 3.09	44.74 ± 2.26
4b	4-Fluoro	22.52 ± 2.04	22.76 ± 5.50	23.69 ± 0.85
4c	2-Chloro	34.57 ± 4.27	43.36 ± 4.61	47.13 ± 3.95
4d	4-Chloro	21.06 ± 1.04	29.25 ± 7.10	45.04 ± 1.02
4e	2-Bromo	42.36 ± 2.58	47.40 ± 4.25	49.96 ± 5.95
4f	4-Bromo	10.74 ± 0.40	18.73 ± 0.88	23.22 ± 1.89
4g	2,4-Dichloro	31.84 ± 1.10	35.81 ± 1.03	49.50 ± 7.14
4h	4-Nitro	50.56 ± 0.70	43.56 ± 7.19	89.92 ± 4.89
4i	4-tolyl	40.22 ± 0.38	33.73 ± 0.84	47.58 ± 8.97
4j	2-Methoxy	71.35 ± 3.74	57.10 ± 5.91	77.81 ± 2.88
4k	4-Methoxy	70.12 ± 2.02	52.85 ± 1.65	76.33 ± 5.66
5a	2-Fluoro	50.74 ± 4.76	60.12 ± 8.43	53.62 ± 4.52
5b	4-Fluoro	61.48 ± 3.28	63.77 ± 2.23	68.78 ± 2.90

Table. *In vitro* cytotoxicity activity of synthesised compounds 4a-k and 5a-1 against selected cancer cell lines.

Compd.	R	IC_{50}(μM)(Mean ±SD)*				
		EGFR	A549	MCF7	HCT116	HEK293
4b	4-Fluoro	28.65 ± 1.96	22.52 ± 2.04	22.76 ± 5.50	23.69 ± 0.85	147.39 ± 4.30
4d	4-Chloro	24.34 ± 1.73	21.06 ± 1.04	29.25 ± 7.10	45.04 ± 1.02	101.03 ± 3.41
4f	4-Bromo	18.35 ± 1.25	10.74 ± 0.40	18.73 ± 0.88	23.22 ± 1.89	96.38 ± 1.79
4g	2,4-Di chloro	35.97 ± 1.89	31.84 ± 1.10	35.81 ± 1.03	49.50 ± 7.14	180.60 ± 5.74
4h	4-Nitro	57.10 ± 0.38	50.56 ± 0.70	43.56 ± 7.19	89.92 ± 4.89	125.01 ± 5.80
4i	4-Methyl	49.65 ± 4.89	40.22 ± 0.38	33.73 ± 0.84	47.58 ± 8.97	146.63 ± 4.57
4k	4-Methoxy	46.47 ± 7.14	70.12 ± 2.02	52.85 ± 1.65	76.33 ± 5.66	163.73 ± 4.69

Table. *In vitro* comparison of cytotoxicity against elected cancer lines, normal cell line and EGFR kinase inhibitory activity of compounds 4b, 4d, 4f-i, 4k, 5d, 5f, 5j, 5l

***In vitro* EGFR inhibitory activity**

All the newly synthesized compounds **4b**, **4d**, **4f-i**, **4k**, **5d**, **5f**, **5j**, **5l** were studied for *in-vitro* EGFR kinase inhibitory activity using solid phase enzyme linked immunosorbent assay (ELISA) method and erlotinib was taken as standard drug. The inhibitory activities (IC_{50}) of the compounds are summarized in Table 8, Figure 61. Among all the tested compounds **4f**,**4d** and **4b** demonstrated potent inhibitory activity with IC_{50} value of 18.35 μM, 24.34 μMand 28.65 μM respectively

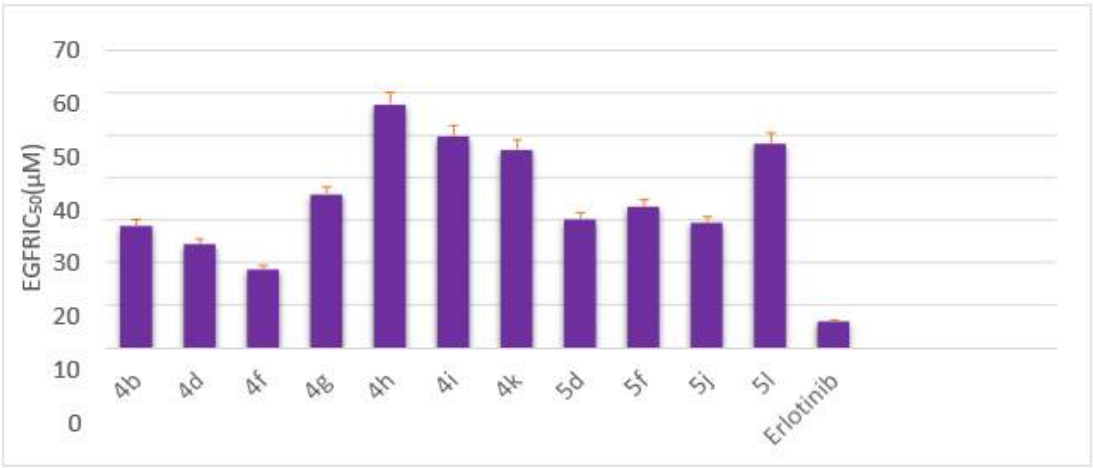

Figure. *In vitro* cytotoxicity demonstrated by (**4b**, **4d**, **4f-4i**, **4k**, **5d**, **5f**, **5j**, **5l**) against EGFR kinase and compared with standard drug Erlo

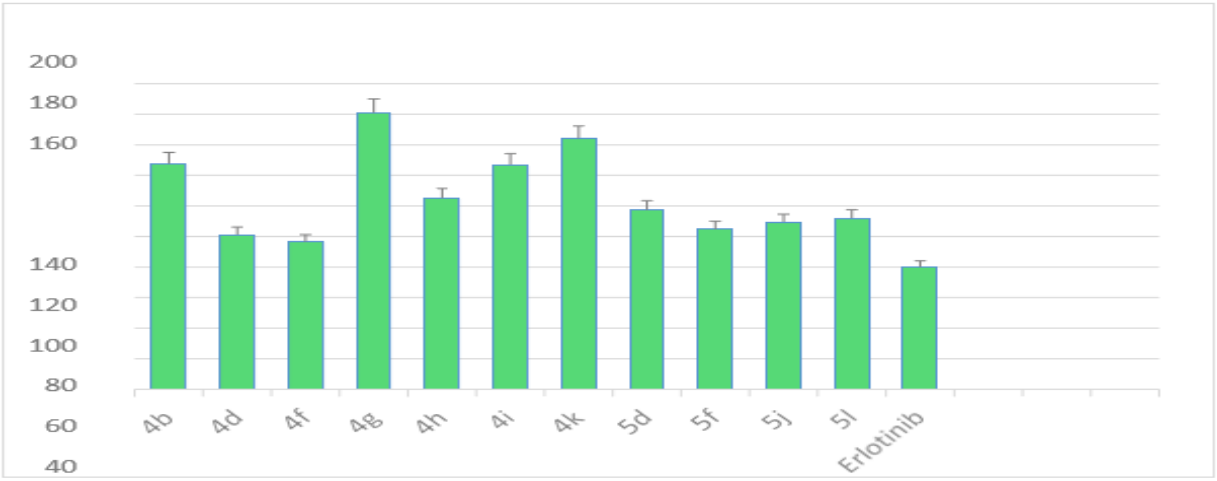

Figure. *In vitro* cytotoxicity demonstrated by (**4b**, **4d**, **4f-i**, **4k**, **5d**, **5f**, **5j**, **5l**) against normal cell line HEK-293 and compared with standard drug Erlotinib

Anti-migratory effect on A549 lung cancer cells

Since cell migration plays an important role in cancer progression and metastasis, a wound-healing assay was conducted to assess the migratory behaviour of A549 cells following treatment with compounds 4b, 4d, and 4f. A scratch was introduced into the confluent cell monolayer using a sterile 200 µL pipette tip, followed by treatment with the compounds at 30 µM. Images of the scratched regions were captured at 0 and 24 h using phase-contrast microscopy. Compared with the untreated control, all three compounds (4b, 4d, and 4f) noticeably reduced the migration of A549 cells into the wounded area, indicating their potential to suppress cancer cell migration.

Nuclear morphological change and nuclear blebbing

A549 cells treated with compounds 4b, 4d, and 4f were examined for nuclear morphological changes using DAPI staining. Compared with untreated cells, the treated cells showed noticeable morphological alterations, including cell shrinkage and membrane blebbing. DAPI staining further revealed chromatin condensation, nuclear fragmentation, and nuclear margination in the treated cells.

Early and late apoptotic cells in A549 cancer cell line

The apoptosis-inducing effects of compounds 4b, 4d, and 4f were investigated in A549 cells using acridine orange/ethidium bromide (AO/EB) dual staining. Compared with the untreated control, the treated cells showed an increased number of apoptotic cells. Both early and late apoptotic changes, along with some necrotic cells, were observed following treatment. These findings suggest that the antiproliferative effects of compounds 4b, 4d, and 4f may be associated with the induction of apoptosis in A549 cells.

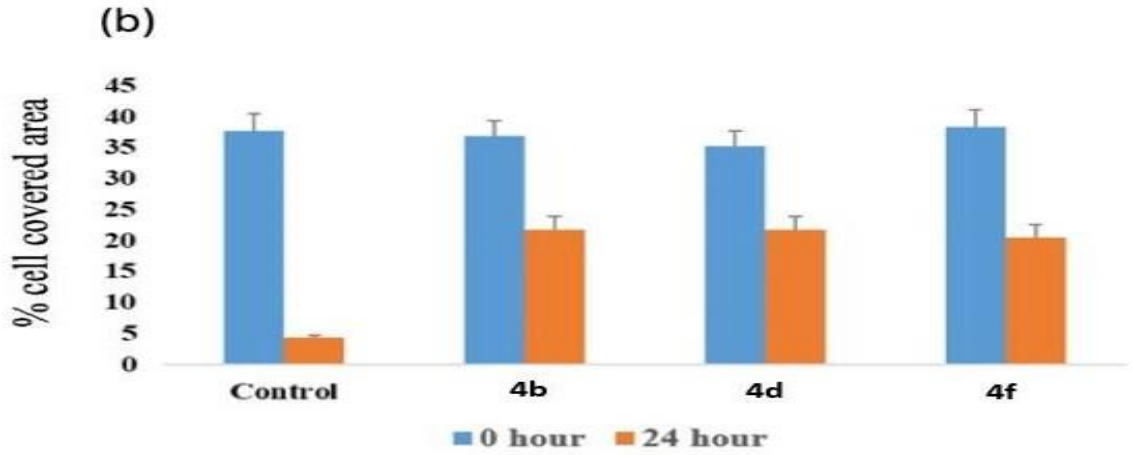

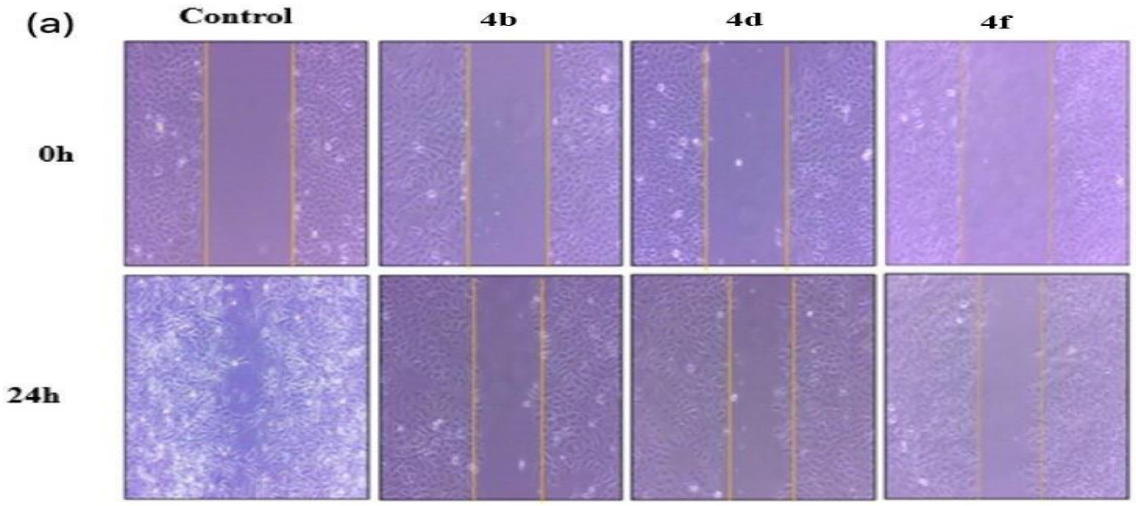

Figure. Wound healing assay of compounds **4b**, **4d and 4f** against A549 cells: (a) The inhibitory effect of compounds **4b**, **4d** and **4f** on A549 cell migration detected by wound healing assay. (b) Representative bar graph showing the cell covered area (%) at 0 and 24h time intervals after treatment with indicated concentration of compounds **4b**, **4d** and **4f**.

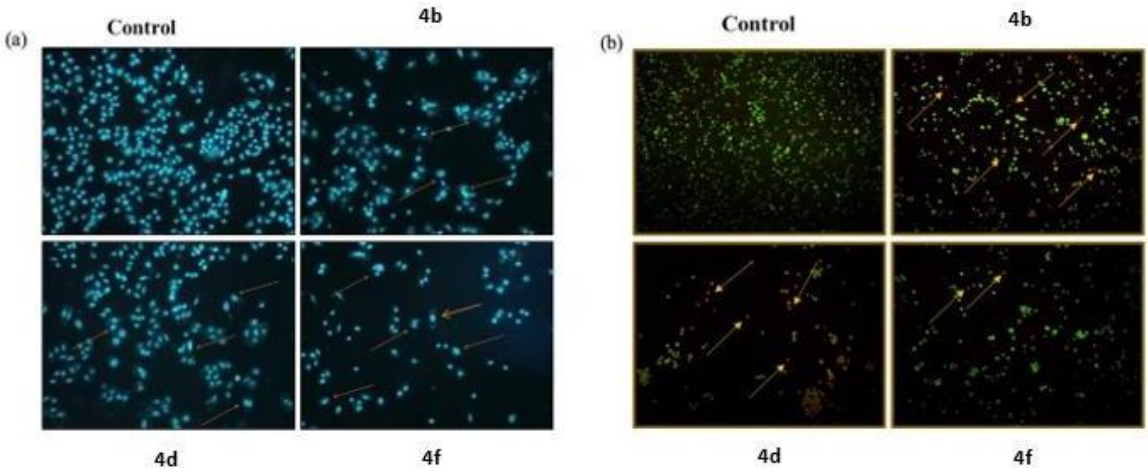

Figure. (**a**)DAPI staining of A549 cells after treatment with compounds **4b**, **4d** and **4f**.

(**b**)AO/EB dual staining of A549 cells after treatment with compounds **4b, 4d** and **4f**.

CONCLUSION

A novel series of imidazothiazole–thiazolidinone hybrid derivatives was designed, synthesized, characterized, and evaluated for their anticancer, EGFR inhibitory, anti-inflammatory, antioxidant, and safety profiles. The synthesized compounds were characterized using IR, ^{1}H NMR, ^{13}C NMR, and mass spectrometry and screened against A549, MCF-7, and HCT116 cancer cell lines. Among the synthesized derivatives, compound 4f showed the most promising anticancer activity, with IC_{50} values of 10.74 ± 0.60 µM against A549 and 18.73 ± 0.88 µM against MCF-7 cells. It also exhibited EGFR inhibitory activity with an IC_{50} of 18.35 ± 1.25 µM. Importantly, 4f showed comparatively lower cytotoxicity toward HEK293 cells (IC_{50} = 96.38 ± 1.79 µM) than erlotinib, suggesting a favorable selectivity profile. Compounds 4d and 4f also demonstrated promising anti-inflammatory activity, producing 84.94% and 83.64% inhibition of albumin denaturation, respectively. Their carrageenan-induced paw edema inhibition was 81.34% and 80.17%, respectively. Both compounds exhibited lower ulcerogenicity and lipid peroxidation than diclofenac sodium. Cardiomyocyte and hepatocyte examinations further indicated no major morphological abnormalities for compounds 4d and 4f. Structure–activity relationship analysis indicated that para-substitution on the N-phenyl ring with

electron-withdrawing groups attached to the thiazolidinone moiety favored anticancer activity. Molecular docking studies with EGFR (PDB ID: 1M17) suggested favorable interactions of compounds 4d and 4f with important active-site residues, including Met769, Cys773, Thr830, Thr766, Lys721, and Asp831, through hydrogen bonding and hydrophobic interactions. Overall, 4f emerged as the lead compound of the series, combining promising anticancer and EGFR inhibitory activities with comparatively lower toxicity toward normal cells. These findings provide a useful structural framework for further optimization and development of more potent imidazothiazole–thiazolidinone-based anticancer agents.

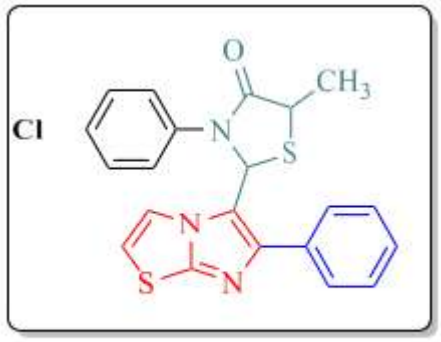

4d

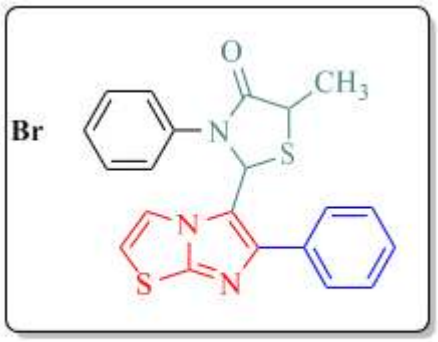

4f

Most active compounds identified from the Synthesized series

REFERENCES

1. Silva FD, Alcorn J J, A Tale of Two Cancers: A Current Concise Overview of Breast And Prostate Cancer. Cancers. 2022;14:2954.
2. Melosky B, Kambartel K, Hantschel M, Bennetts M, Nickens D, Brinkmann J, Kayser A, Moran M, & Cappuzzo F. Worldwide Prevalence of Epidermal Growth Factor Receptor Mutations in Non-Small Cell Lung Cancer: A Meta-Analysis. Molecular Diagnosis & Therapy. 2022; 26: 18.
3. Islami F, Guerra CE, Minihan A, Yabroff KR, Fedewa SA, Sloan K, Wiedt TL, Thomson B, Siegel RL, Nargis N, Winn RA, Lacasse L, Makaroff L, Daniels EC, Patel AV, Cance WG, Jemal A. American Cancer Society's report on the status of cancer disparities in the United States, CA Cancer J. Clin. 2022; 72: 112-143.
4. Ferlay J, Colombet M, Soerjomataram I, Parkin DM, Piñeros M, Znaor A, Bray F. Cancer statistics for the year 2020: An overview. Int. J. Cancer 2021; 149: 778-789.
5. HaiderK,Das S, Joseph A,YarM S. Anappraisal ofanticancer activitywith structure– activity relationship of quinazoline and quinazolinone analogues through EGFR and VEGFR inhibition: A review. Drug Dev. Res 2022; 83: 859-890.
6. JaziehAR, Alkaiyat M, Abuelgasim KA, Ardah H. Them trends of cancer patients' perceptions on the causes and risk factors of cancer over time. Saudi Med. J 2022; 43: 479-485.
7. SangamithraA,TheCausesofCancer:AnAnalysisofAvoidableRiskFactors.Shanlax Int. J. Econ 2021; 9: 37-40.
8. Haider K, Shrivastava N,Pathak A, Dewangan RP, Yahya S, Yar MS. Recent advances and SAR study of 2-substituted benzothiazole scaffold based potent chemotherapeutic agents. Results Chem 2021; 4: 100258.
9. SharmaP, LaRosaC, Antwi J, Govindarajan R,Werbovetz KA. Imidazoles as potential anticancer agents: An update on recent studies. Molecules 2021; 26: 4213.
10. London M, Gallo E. Epidermal growth factor receptor (EGFR) involvement in epithelial derived cancers and its current antibody-based immunotherapies. Cell Biol. Int. 2020; 44:1267-1282.
11. SinghD, AttriBK, GillRK, BariwalJ. Review on EGFR Inhibitors: Critical Updates. MiniRev.Med. Chem2016;16: 1134-1166.
12. Soltan OM, Shoman ME, Abdel-Aziz SA, Narumi A, Konno H, Abdel-Aziz M. Molecular hybrids: A five-year survey on structures of multiple targeted hybrids of protein kinase inhibitors for cancer therapy. Eur. J. Med. Chem 2021; 225: 113768.

13. Tay RY, Wong R, Hawkes EA. Treatment of metastatic colorectal cancer: Focus on panitumumab. Cancer Manag. Res. 2015; 7: 189-19810.
14. Quesnelle KM, Boehm AL, Grandis JR. STAT-mediated EGFR signaling in cancer. J. Cell. Biochem 2007; 102: 311-319.
15. Hossam M, Lasheen DS, Abouzid KAM, Covalent EGFR Inhibitors: Binding Mechanisms, Synthetic Approaches, and Clinical Profiles. Arch. Pharm 2016; 349: 573–593.
16. Uribe ML, Marrocco I, Yarden Y. EGFR in Cancer: SignalingMechanisms, Drugs, and Acquired Resistance. Cancers 2021; 13: 2748.
17. Takeuchi O, Akira S. Pattern Recognition Receptors and Inflammation. Cell 2010; 140: 805-820.
18. ChertovO, Yang D, Howard O, Oppenheim JJ. Leukocyte granule proteins mobilize innate host defenses and adaptive immune responses. Immunol Rev 2000; 177: 68-78.
19. Jabbour HN, Sales KJ, Catalano RD, Norman JE. Inflammatory pathways in female reproductive health and disease. Reprod 2009; 138: 903-919.
20. MedzhitovR,JanewayCJr.Innate immunity.N EnglJMed 2000;343: 338-44.

HOW TO CITE: Sakshi*, N. S. Gill, Surinderjeet Kaur, A Research On Design And Synthesis Of Fused Heterocyclic Imidazothiazole And Benzothiazole Analogous As Potential Anti-Cancer Agents, Int. J. Sci. R. Tech., 2026, 3 (9), 89-102. https://doi.org/10.5281/zenodo.22303144